Electronic Supplementary Material (ESI) for Nanoscale.

Supplementary Material

Electrically and optically erasable non-volatile two-dimensional electron gas memory

Dongxing Zheng[1, 2], Junwei Zhang[1, 3], Xin He[1], Yan Wen[1], Peng Li[1, 4], Yuchen Wang[2], Yinchang Ma[1], Haili Bai[2], Husam N. Alshareef[1], XiXiang Zhang[1*]

1 King Abdullah University of Science and Technology (KAUST), Physical Science and Engineering Division (PSE), Thuwal 23955-6900, Saudi Arabia

2 Tianjin Key Laboratory of Low Dimensional Materials Physics and Processing Technology, Institute of Advanced Materials Physics, Faculty of Science, Tianjin University, Tianjin 300354, P. R. China

3 Key Laboratory of Magnetism and Magnetic Materials of Ministry of Education, School of Physical Science and Technology, Lanzhou University, Lanzhou,730000, P. R. China

4 State Key Laboratory of Electronic Thin Film and Integrated Devices, University of Electronic Science and Technology of China, Chengdu 610054, P. R. China

[*]Author to whom all correspondence should be addressed

E-mail: xixiang.zhang@kaust.edu.sa

METHODS

Sample fabrication:

The LAO films were grown via pulsed laser deposition on 0.5-mm-thick 5 × 5 mm^2 TiO_2-terminated (001)-oriented STO substrates. To realize TiO_2-termination, the STO substrates were first etched by Buffered HF for 10 s. The substrates were then annealed in a tube furnace at 1000 ^oC with an O_2 partial pressure of 60 Torr for 1 h. Following this process, the TiO_2-termination was achieved, which was confirmed based on surface morphology measurements via AFM. A single-crystal LAO target was ablated by a KrF (248 nm) excimer laser at a repetition rate of 3 Hz and fluence of 1.5 J/cm^2. During the deposition, the substrate temperature was maintained at 750 ^oC with an oxygen partial pressure of 6.0×10^{-6} Torr. After the growth of the LAO film, the samples were annealed for 30 min at an oxygen pressure of 1 Torr at 500 ^oC. Finally, the LAO/STO heterostructures were cooled at 25 ^oC/min while maintaining the same oxygen pressure.

Characterization of Structure and Physical Properties:

Monochromated Cs-corrected high-resolution scanning transmission electron microscopy (STEM, Titan 80-300, FEI) was performed to characterize the interfacial structure. The STEM sample was prepared using a focused ion beam (FIB) (Helios 450, FEI). The samples were electrically contacted with aluminum wires (20 μm in diameter) via ultrasonic wedge bonding. The electrical transport properties were measured using a Quantum Design Dynacool system combined with a Keithley 2636 source meter, 6221 current source, and 2182 voltage meter. The gating voltage was applied on the bottom side of the STO substrate while the top surface of the LAO substrate was kept grounded. To obtain the R-V curves, the resistance was measured in a two-point configuration with a source current of 1 μA, because at the high resistance state, the resistance was too high to produce a steady voltage between the two voltage contacts of the

four-point setup. Corresponding to the insulating state, the resistance exceeded the 200 MΩ measurement range of a multimeter. Light was introduced into the chamber of the Dynacool system via an optical fiber. The temperture dependent capacitance curves of STO substrate were measured by Hikoi IM3536 LCR meter combined with the Quantum Design Physical Properties Measurement System.

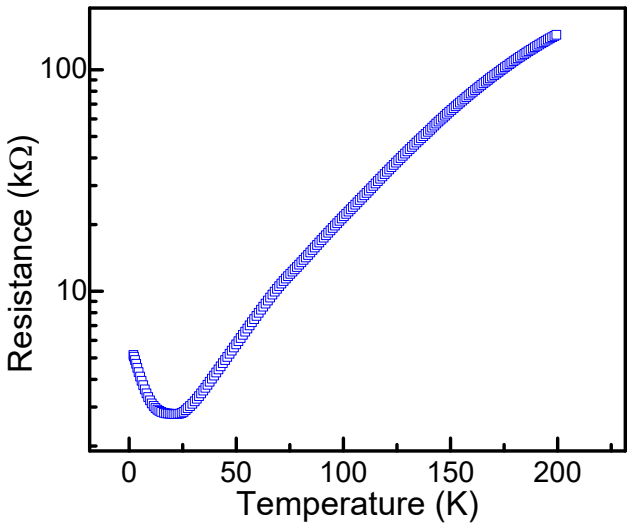

Figure S1: Temperature dependence of resistance measured for the LAO(6 uc)/STO heterostructure.

The resistance firstly decreases with the decreasing temperature. This is corresponding to a metallic transport behavior. However, when the temperature was below 20 K, the resistance increases with the decreasing temperature, which can be attributed to both the Kondo effect[1] and weak localization[2].

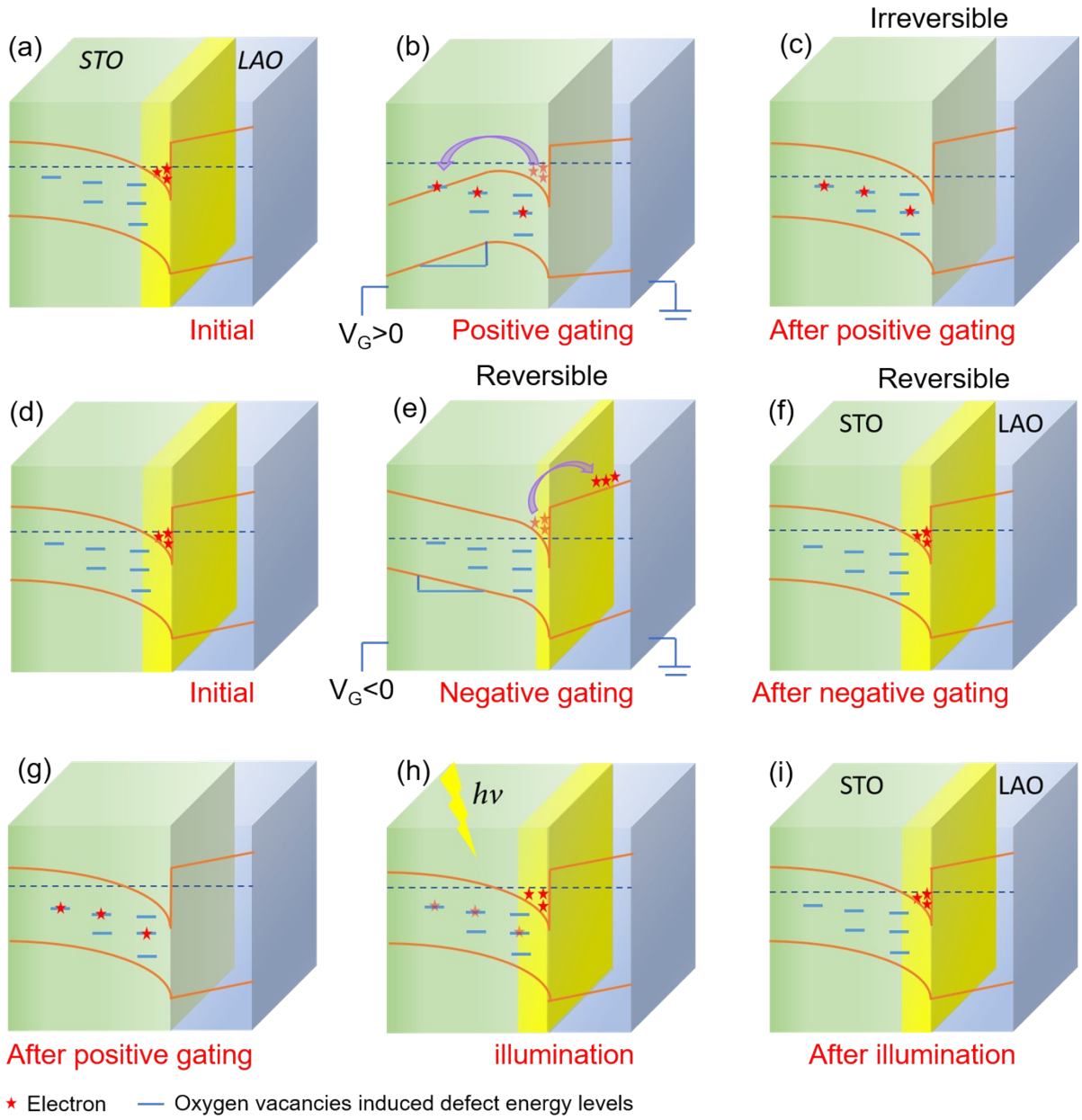

Figure S2: Metal-insulator transition mechanism. Schematic drawings of the LAO/STO 2DEG system and corresponding potential energy profiles for the positive voltage gating process (a) initial, (b) during positive voltage gating, and (c) after positive voltage gating. Negative voltage gating process (d) initial, (e) during negative voltage gating, and (f) after negative voltage gating. The illumination process (g) after the positive voltage gating process, (h) during illumination and (i) after illumination. The arrows schematically show the jumping direction of the electron.

As shown in Figure S2a, for the initial state, the oxygen vacancies induced defect erengy levels are slightly below the Fermi energy level and the electron is confined at the 2DEG QW, at this time, the sample exhibits a normal metallic 2DEG transport behavior. In Figure S2b, when a large enough positive voltage is applied at the gate, the conduction band is bent down and the electron from the 2DEG QW escape to the defect energy levels induced by oxygen

vacancies. After the removal of the applied voltage, the conduction band will recover to its original position and shape, while the electrons cannot go back to the 2DEG QW and they remain in the defect energy level due to the energy gap between them. Thus, after applying a large enough positive pulse voltage, the electrons in the 2DEG are emptied, which leads to an insulating state. This process is irreversible as shown in Figures S2 a-c. When a negative gating pulse is applied, as shown in Figures S2d-f, the process is reversible. Firstly, the electrons in the quantum well are extracted to the conduction band in LAO by the applied electric field due to the conduction band is lowered by the negative gating, which makes the sample insulating. However, once the gating voltage is turned off, the conduction band will recover to its original shape and position. As the oxygen vacancy formation energy of LAO is much larger than STO[3-5], the electrons cannot be retained in the LAO layer and they return to the 2DEG QW easily. Then the sample recovers to its metallic state.

Figures S2g-i schematically show the process of switching the insulating state caused by a large enough positive pulse gating voltage to a conducting state after light illumination. As shown in Figure S2g, after the positive gating pulse, the sample becomes insulating as we described in Figures S2a-c. Under light illumination, the electrons will absorb the photon energy to overcome the energy gap between the defect energy level and the energy level of the 2DEG QW through the electron-photon interaction. Then the sample recovers to its conducting state.

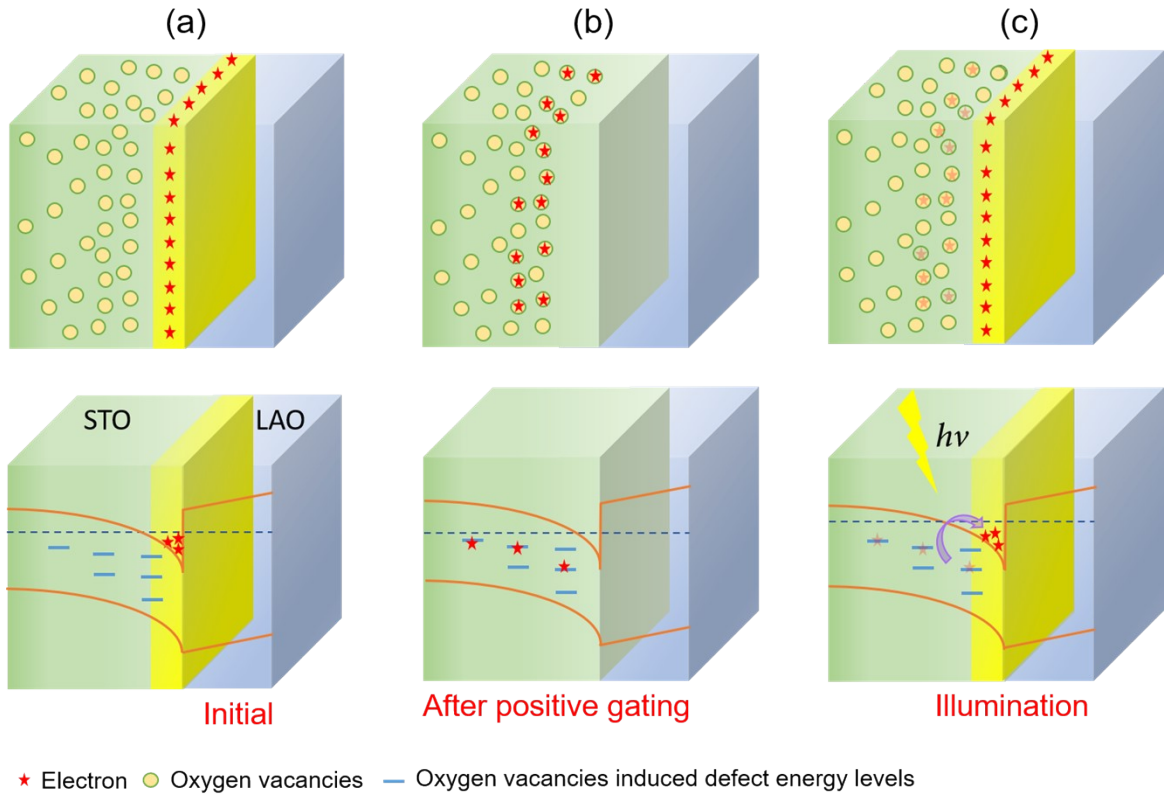

Figure S3: Metal-insulator transition mechanism. Schematic illustration of the trapping mechanism and band diagram of the LAO/STO interface under influence of voltage gating and optical illumination. (a) Initial, (b) After positive voltage gating and (c) illumination states.

Schematic illustration of the trapping mechanism and band diagram of the LAO/STO interface under influence of voltage gating and optical illumination is in Fig. S3. In the initial state, the free electrons are mainly restricted in the 2DEG quantum well. During the positive voltage gating process, the conduction band is bent down and the electrons from the 2DEG QW escape to the defect energy levels induced by oxygen vacancies. After the removal of the applied voltage, the conduction band will recover to its original position and shape, while the electrons cannot go back to the 2DEG QW and become localized. A delocalization process can be realized by optical illumination, in which the localized electron can hop to the 2DEG quantum well by absorbing a photon.

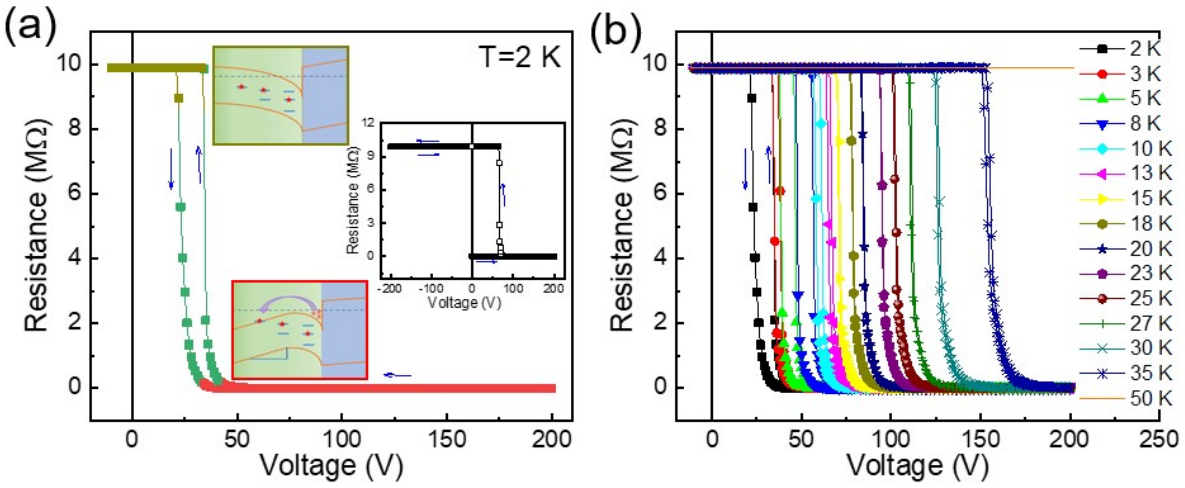

Figure S4: *R-V* curves of the LAO/STO heterostructure measured at different temperatures after a positive pulse voltage (200 V, 300 ms) pre-gating process. Voltage sweeps from 0 V→200 V →-10 V→ 0 V, the direction is indicated by the blue arrows, 10 MΩ corresponds to the measurement limit with the current source of 1 uA, and the maximum measure voltage of 10 V for the voltage meter. (a) *R-V* curve at 2 K, the corresponding band structure is schematically shown in the bottom and top insets for the ON and OFF states, respectively. (b) Temperature dependent *R-V* curves of the LAO/STO heterostructure.

As shown in Figures S2a-c, the sample was tuned to an insulating state when it was pre-gated by a positive pulse voltage. During the measurement of the *R-V* curves, *R* was measured by sweeping V_g with a step of 1 V. In Figure S4a, with the increase of voltage from 0 V, the sample maintains the insulating state till to the critical voltage V_g=40 V. Above the critical value, the resistance decreases sharply with the increasing voltage and reaches a value of ~ 100 Ω **at** V_g **=200 V**. The positive pulse voltage pre-gating process just turns the sample to an insulating (OFF) state. To turn the sample to the conducting (ON) state, a voltage that is much larger than the critical voltage has to be applied. From Figure S4b, we can see that the critical voltage strongly depends on temperature and it increases with the increasing temperature. Two mechanisms account for this phenomenon. Firstly, a higher temperature facilitates the electrons to re redistribute more quickly when the gating voltage was removed. Secondly, the permittivity

of the STO substrate decreases with the increasing temperature[4, 5], which leads to a weaker bonding of the electron.

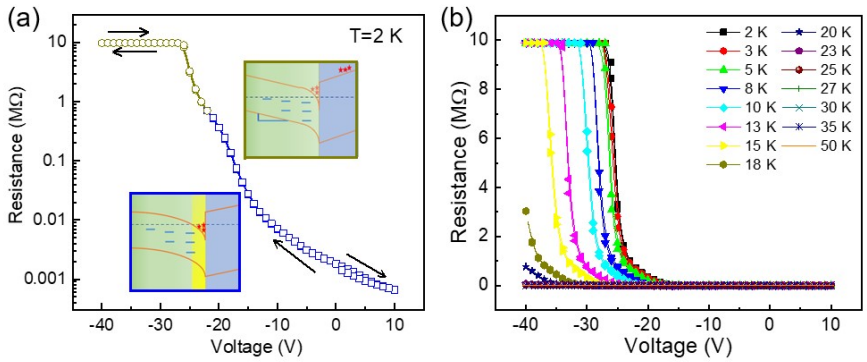

Figure S5: *R-V* curves of the LAO/STO heterostructure after a negative pulse voltage (-40 V, 300 ms) pre-gating process at different temperatures. Voltage sweeps from 0 V→-40 V →10 V→ 0 V (. (a) *R-V* curve at 2 K. The corresponding band structure is shown schematically in the bottom-left and top-right insets for the ON and OFF states, respectively. (b) Temperature dependent *R-V* curves of the LAO/STO heterostructure.

The negative pulse voltage pre-gating process does not have much influence on the resistance state. Unlike the situation of the positive pulse voltage gating process, it maintains the metallic state. As schematically shown in Figure S2e, the negative voltage will raise STO's conduction band and drive the electron away from the 2DEG QW to the LAO layer. As the oxygen vacancy formation energy in LAO is much higher than that in the STO, it is quite difficult to form the defect energy level induced by oxygen vacancies in the LAO layer[3, 6, 7]. Moreover, the only 6 uc thickness of the LAO film also makes it difficult to store the electrons. Thus the electrons in the 2DEG cannot be stored in the LAO layer, and they will return to the 2DEG QW when the negative voltage is removed (see Figure S2g), which should lead to a reversible behavior. As shown in Figure 3b, for the negative polarization process (voltage from 0 V→-40 V →10 V→ 0 V), the resistance increases rapidly with the increasing negative voltage and reaches the measurement limit after a threshold voltage. By decreasing the negative voltage, the resistance firstly maintains the insulating state and then drops quickly after the threshold

voltage is reached. The forward and backward curves overlap with each other, indicating a reversible process.

The temperature dependent negative polarization process is shown in Figure S5b, a reversible metal-insulator transition behavior was also observed. The threshold voltage of the metal-insulator transition increases with the increasing temperature, which is due to the decrease of the permittivity of the STO substrate with the increasing temperature[4, 5] and the enhanced thermal energy with the increasing temperature[8].

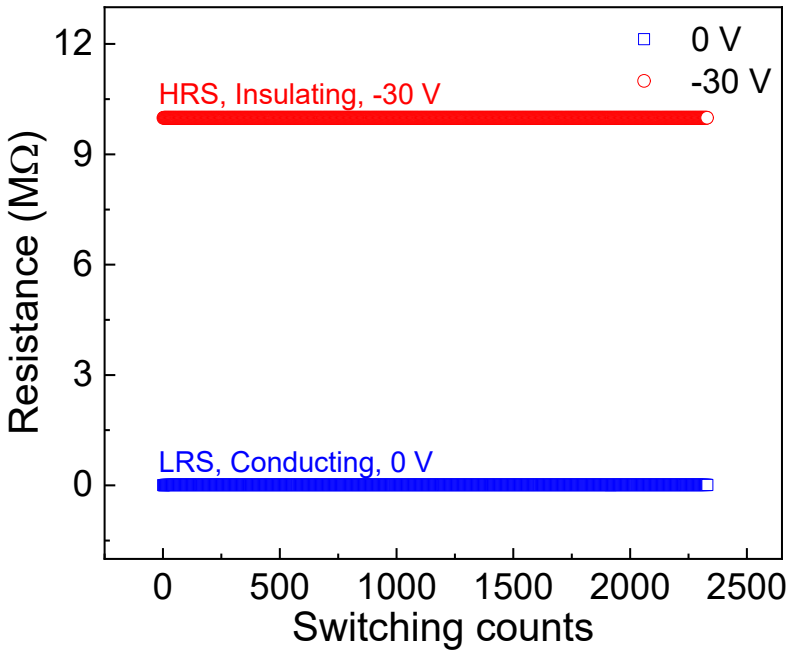

Figure S6: Reversible switching of the High resistance state (HRS) and Low resistance state (LRS) at 3 K.

In contrary to an insulating state after the positive pulse voltage pre-gating process in Figure S4, the negative pulse voltage pre-gating process does not have much influence on the band structure of the sample as the electron will return to the 2DEG QW when the voltage is removed. So it is the same to pre-gate the sample with a negative pulse voltage or without pre-gating process. Figure S6 shows the reversible switching of the resistive state without the pre-gating process. For the initial state, the sample is conducting without the applying of voltage. When a negative voltage of -30 V was applied, the sample was tuned to an insulating state. After the removal of the voltage, the sample becomes conducting again. After thousands of times of switching, the HRS and LRS states are robust without any fatigue behavior.

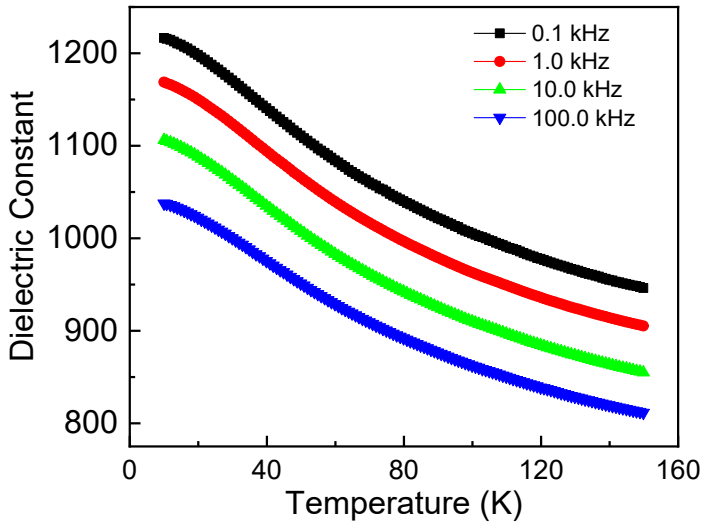

Figure S7: Temperature dependent dielectric constant of STO substrate measured with different frequency.

The temperature dependent dielectric constant of STO substrate was measured by the Hikoi IM3536 LCR meter combined with the Quantum Design Physical Properties Measurement System. An AC voltage of 1 V with the frequency of 0.1, 1, 10, and 100 kHz was applied during measurement. The STO substrate was first cooled from room temperature to 10 K, then the capacitance of the STO substrate was measured during the warming process. The STO substrate shows a phase transition from cubic to tetragonal structure at 105 K, which may have an influence on the avalanche-like drop of resistance shown in Figure 3a. However, no abnormal change of dielectric constant was discovered during the whole temperature range, thus we can conclude that the avalanche-like drop resistance is induced by the thermally assisted jumping of electrons from the defect energy level to the 2DEG QW.

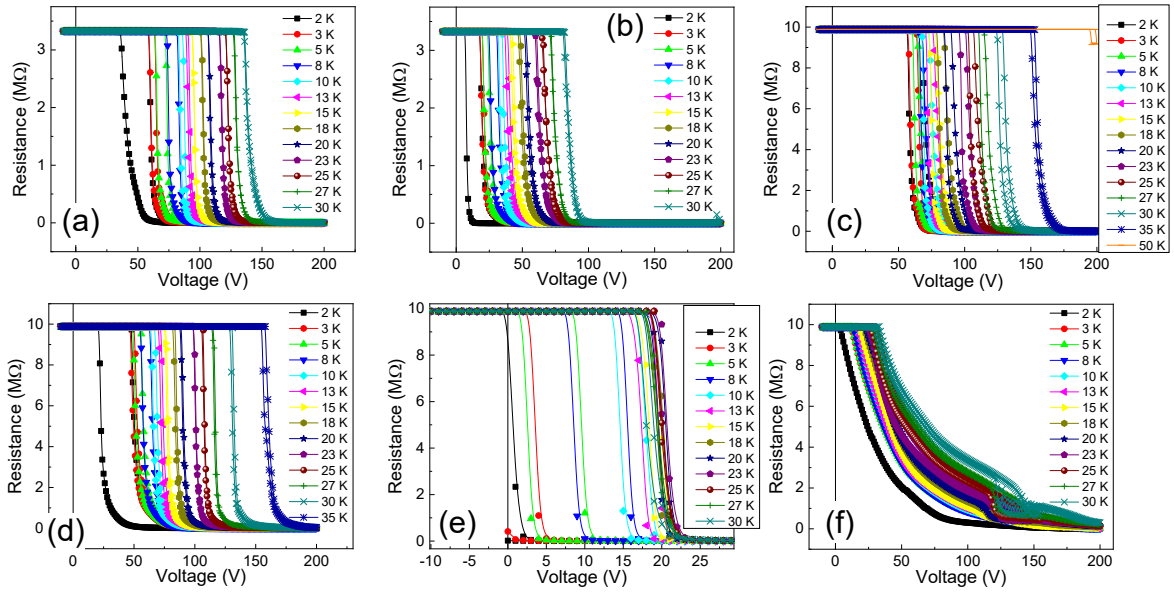

Figure S8: *R-V* curves of the sample with LAO thickness of 6 uc and annealed at (a) 60 Pa, (b) 80 Pa, (c) 100 Pa, (d) 120 Pa and (e) 300 Torr. (f) *R-V* curve of sample with LAO thickness of 10 uc and annealed at 133 Pa.

The *R-V* curves of the sample with LAO thickness of 6 uc and annealed at different oxygen pressure is shown in Figures S8a-e. The sample was fabricated at 750 °C with an oxygen partial pressure of 6.0×10^{-6} Torr. After the deposition, the temperature was decreased to 500 °C and the samples were annealed with various oxygen pressure. A reversible modulation between the conducting and insulating states was achieved in all the samples except for the different of critical voltage. As mentioned in the manuscript, the conducting state modulated by the gating voltage is related to the band bending of STO substrate,which leads to an overlap of the deffect energy level and the conduction band of STO substrates. Here, the differences between the critical voltage may due to the randomly formation of oxygen vacancies in the samples. In Fig. S8 (f), when the LAO thickness was increased to 10 uc, a reversible modulation between the conducting and insulating states was also achieved.

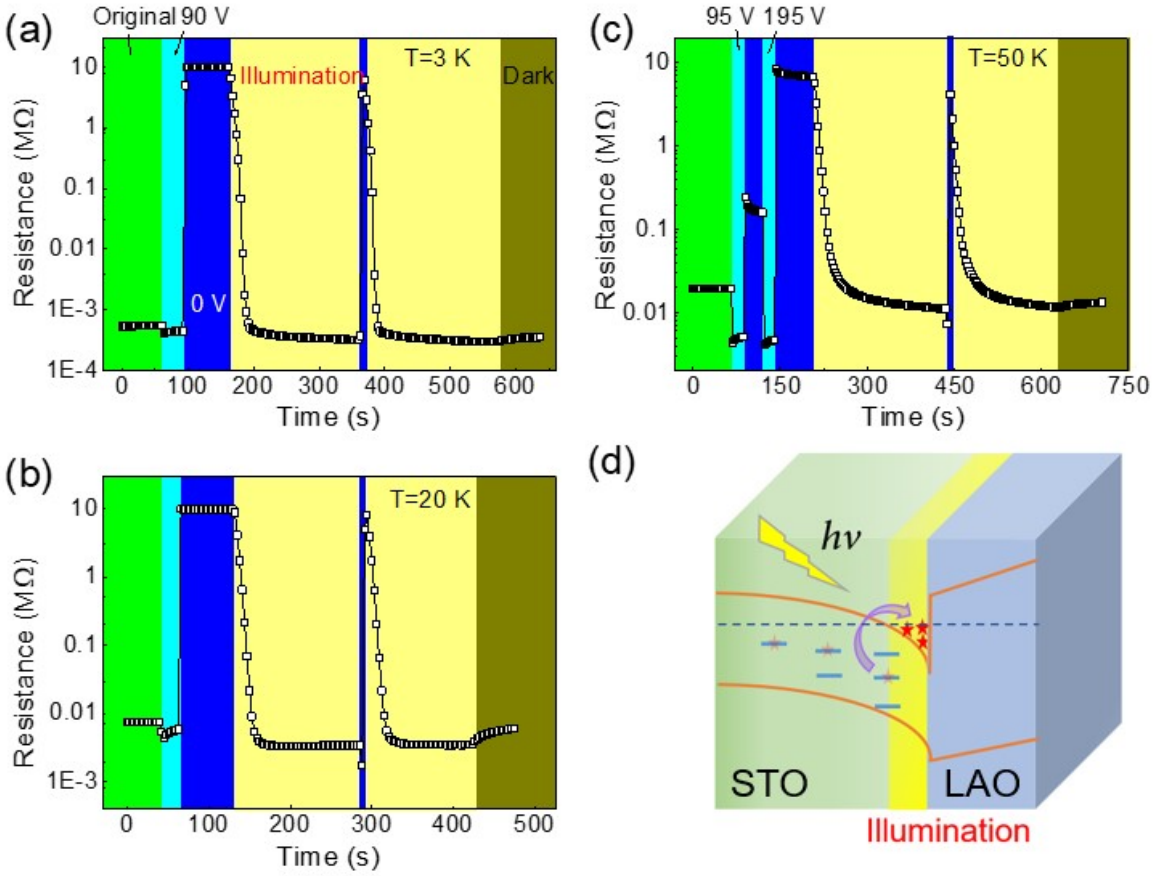

Figure S9: Effect of illumination a) Illumination and voltage gating co-modulated metal-insulator transition at (a) *T*=3 K, (b) *T*=20 K, and (c) *T*=50 K. (d) Schematic drawing of the illumination effect on the insulator to the metal transition process.

Figures S9a-c show the influence of white light (wavelength of 400~740 nm) illumination on the resistance states. The measurement was performed at 3, 20, and 50 K. The green zone shows the resistance of the initial metallic state. With the application of a 95 V voltage, the sample becomes more conducting. After the removal of V_g, it becomes insulating. It maintains the insulating state unless the sample is illuminated. From the yellow region (under the illumination), we can see that the resistance drops sharply, and the sample transfer to the metallic state after 20 seconds. During the illumination process, a 95 V voltage with the duration of 1 s was applied at *t*=~370 s, the sample was tuned to the insulating state again. But this state is not stable in the illumination condition, it returns to the metallic state again in 20 s after the removal of gating voltage.

In Figure S9c, at 50 K, the thermal activation energy was enhanced and the voltage of 95 V is not sufficient to tune the sample into an insulating state. A 195 V voltage was applied to further tune it into an insulating state. As schematically shown in Fig. S8d, the trapped electron will be excited when it absorbs a photon. We also note that when the illumination is removed, the resistance increases slightly (dark region) for all the three temperatures. This effect can be ascribed to a relaxation process by the thermal effect induced electron hooping. As shown in Figures S9a-c, the sample in the illumination condition becomes more conducting as compared to the initial state. This is due to the illumination, which activates more electron from the defect induced donor center to the 2DEG quantum well. It is not a stable state when the illumination is removed, thus the resistance increases gradually but lower than the initial state.

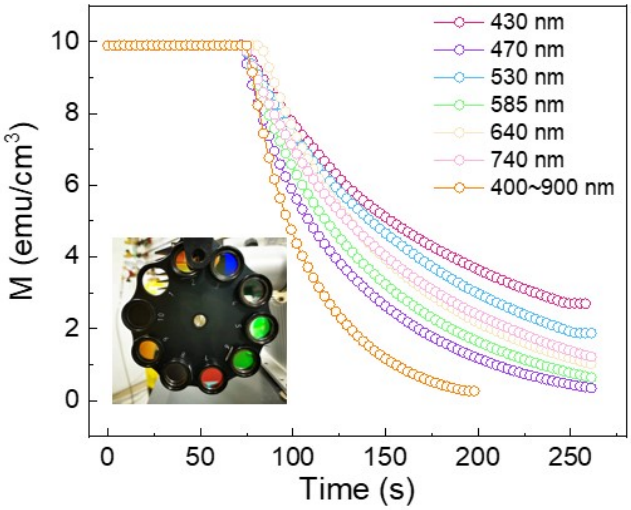

Figure S10: Time dependence of resistance, *R-t* curves, under illumination with the light of different wavelengths. The inset shows the optical filter to select the desired wavelength.

The light with different wavelengths was applied to modulate the resistance of the samples between the conducting and insulating states. The light with different wavelengths was achieved by using the optical filters shown in the inset of Fig. S10. The infrared light with the longest wavelength of 740 nm (E=1.68 eV) is also able to drive the state from insulating to conducting, which indicates that the energy gap between the 2DEG QW and defect energy level is less than 1.68 V. This result is consistent with Baeumer's study that the defect energy level is determined to be lower than the conduction band with the value between 0.31 to 1.10 eV at low temperatures[8].

References

[1] A. Brinkman, M. Huijben, M. Van Zalk, J. Huijben, U. Zeitler, J. C. Maan, W. G. Van der Wiel, G. Rijnders, D. H. A. Blank, H. Hilgenkamp, Nature Mater. **6**, 493 (2007)., Nature Mater. **6**, 493 (2007).
[2] A. D. Caviglia, M. Gabay, S. Gariglio, N. Reyren, C. Cancellieri, and J. M. Triscone, Phys. Rev. Lett. **104**, 126803 (2010).
[3] Y. Li, S. N. Phattalung, S. Limpijumnong, J. Kim, and J. Yu, Phys. Rev. B **84**, 245307 (2011).
[4] J. Park, B.-G. Cho, K. D. Kim, J. Koo, H. Jang, K.-T. Ko, J.-H. Park, K.-B. Lee, J.-Y. Kim, D. R. Lee, C. A. Burns, S. S. A. Seo, H. N. Lee, Phys. Rev. Lett. **110**, 017401 (2013).
[5] O. Okhay, A. Tkach, A. Wu, and P. M. Vilarinho, J. Phys. D: Appl. Phys. **46**, 505315 (2013).
[6] W. Siemons, G. Koster, H. Yamamoto, W. A. Harrison, G. Lucovsky, T. H. Geballe, D. H. A. Blank, and M. R. Beasley, Phys. Rev. Lett. **98**, 196802 (2007).
[7]A. Kalabukhov, R. Gunnarsson, J. Börjesson, E. Olsson, T. Claeson, and D. Winkler, Phys. Rev. B **75**, 121404 (2007).
[8]Y. Chen, Y. Lechaux, B. Casals, B. Guillet, A. Minj, J. Gázquez, L. Méchin, and G. Herranz, Phys. Rev. Lett. **124**, 246804 (2020).